

## Solar cell power generation modeling

Shivali Kulshrestha<sup>1\*</sup>, M.K. Bhaskar<sup>2</sup>

<sup>1</sup>*M.E. Student, Department of Electrical Engineering, M.B.M. Engineering College, J.N.V. University,  
Jodhpur-342001, Rajasthan, India*

<sup>2</sup>*Associate Professor, Department of Electrical Engineering, M.B.M. Engineering College, J.N.V. University,  
Jodhpur-342001, Rajasthan, India*

\*\*\*

**Abstract** –A Photovoltaic (PV) system directly converts sunlight into electricity. The basic device of a PV system is the PV cell. PV cells are made of semiconductor material such as silicon. When light energy strikes the solar cell, electrons are knocked loose from the atoms in the semiconductor material. If electrical conductors are attached to the positive and negative sides, forming an electrical circuit, the electrons can be captured in the form of an electric current. This electricity can then be used to power a load. In this paper, we describe PV solar cell power generation modeling of the spacecraft. The obtained solar cell governing equation is solved by the well known Newton-Raphson method numerically.

primarily the non-linear current-voltage relationship of the solar cell. The problem of interfacing with the non-linear relationship is exacerbated by the fact that the relationship is dependent on multiple parameters including total radiation fluence, incident angle with respect to the Sun, and temperature. Despite these difficulties there are various techniques that optimize the interface to the PV system and allow for maximum power generation at the expense of circuit board area, complexity, and, in some instances, decreased overall system efficiency.

The electrical power system generates, stores, conditions, controls, and distributes power within the specified voltage band to all bus and payload equipment. The protection of the power system components in case of all credible faults is also included. The basic components of the power system are the solar array, solar array drive, battery, battery charge and discharge regulators, bus voltage regulator, load switching, fuses, and the distribution harness. The harness consists of conducting wires and connectors that connect various components together.

In the Earth orbiting spacecraft, the solar array is rotated once per orbit by the solar array drive to track the sun at or near normal angle. The rotation is rate-servo controlled. The body information and position errors are computed by the satellite computer to derive rate control signals. The nominal rate of rotation is 0.06 degree per second. Using slip rings and carbon brushes is one way of providing the rotary joint between the rotating array and the satellite body. The control signals for required rotation rate come from the Telemetry, Tele-command & Control (TTC) system, which also selects the rotation direction.

Photovoltaic (PV) system directly converts sunlight into electricity. The basic device of a PV system is the PV cell. A set of connected cells form a panel. Panels are generally composed of series cells in order to obtain large output voltages. Panels with large output currents are achieved by increasing the surface area of the cells or by connecting cells in parallel. A PV array may be either a panel or a set of panels connected in series or parallel to form large PV systems (Villalva et al. 2009). PV cells are made of semiconductor materials, such as silicon. When light

**Key Words:** Solar cell, mathematical model, Newton-Raphson method, characteristic curves.

### 1. INTRODUCTION

The most important system on-board any spacecraft is its electrical power system as every other subsystem requires power to operate. The ability to generate power is necessary for all but the simplest spacecraft. While missions with low average power consumption and lifetimes on the order of weeks can survive simply on primary batteries, any mission that must last longer or work harder must be able to constantly generate energy or replenish stored energy to be used later. There are many options for power generation that have been successfully used in spacecraft including fuel cells and nuclear-thermoelectric, however, by far the most widely used power generation technology for spacecraft is photovoltaic (PV). Furthermore, given the relative size, design constraints, and expense of the more exotic solutions, PVs are practically the only option for the vast majority of missions. PV array consists of number of solar panel substrates on which solar cells are laid down in series and parallel for its power requirement generation.

There are several operating characteristics of PVs that must be considered when designing a photovoltaic system,

energy strikes the solar cell, electrons are knocked loose from the atoms in the semiconductor material. If electrical conductors are attached to the positive and negative sides, forming an electrical circuit, the electrons can be captured in the form of an electric current, i.e., electricity. This electricity can then be used to power a load. Due to the low voltage generated in a PV cell ( $\sim 0.5V$ ), several PV cells are connected in series (for high voltage) and in parallel (for high current) to form a PV module for desired output, as shown in Fig. 5.9. The power that one module can produce is not sufficient to meet the requirements of the spacecraft. Most PV arrays use an inverter to convert the DC power into alternating current that can power the spacecraft's motors, loads etc. The modules in a PV array are usually first connected in series to obtain the desired voltages; the individual modules are then connected in parallel to allow the system to produce more current (Pachpande and Zope, 2012).

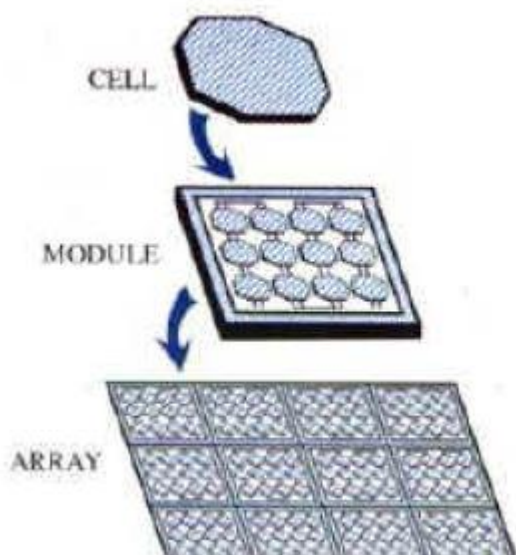


**Fig. 1:** Photovoltaic system (Pachpande and Zope, 2012).

## 2. MATHEMATICAL MODEL

Solar cell is made of large area semiconductor diodes. Due to photovoltaic effect energy of light (energy of photons) converts into electrical current. The simplest equivalent electrical circuit of a solar cell is a shown in Fig. 2. The circuit parameters are as follows. The series resistance,  $R_s$ , represents the internal resistance to the current flow. It is primarily due to the resistivity of the material. The shunt resistance,  $R_{sh}$ , represents the leakage current across the junction. It depends on the p-n junction depth, the impurities, and the contact resistance. The value of  $R_{sh}$  is inversely related with the leakage current to ground. In an ideal PV cell,  $R_s = 0$  (no series loss), and

$R_{sh} = \infty$  (no leakage to ground). In a typical high quality  $2.5 \times 2.5 \text{ cm}^2$  silicon cell,  $R_s = 0.05$  to  $0.10 \text{ ohm}$  and  $R_{sh} = 200$  to  $300 \text{ ohm}$  (Patel 2005).

The output of the current source is directly proportional to the light falling on the cell. When the spacecraft is in dark side of the Earth, the solar cell is not an active device; it works as a diode, i.e., a p-n junction. It produces neither a current nor a voltage. However, if it is connected to an external supply (large voltage) it generates a current  $I_d$ , called diode ( $D$ ) current or dark current.

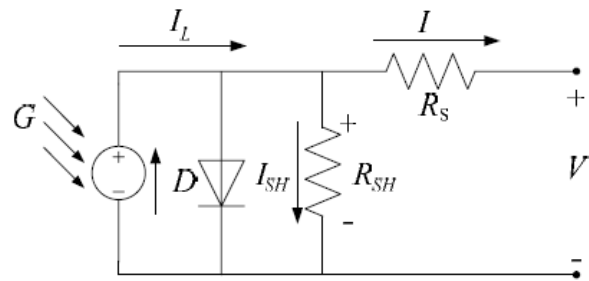


**Fig. 2:** Electrical circuit diagram of PV cell (González-Longatt 2005).

The diode current,  $I_d$ , is given by the classical diode current expression (Sanchez et al., 1996; Awodugba et al. 2013):

$$I_d = I_0 \left[ \exp\left(\frac{V_d}{aV_t}\right) - 1 \right], \quad (1)$$

where  $I_0$  is the reverse saturation current,  $a$  is the diode quality factor,  $V_d$  is the diode voltage,  $V_t$  is the thermal voltage ( $V_t = 27.5 \text{ mV}$  at  $25^\circ\text{C}$ ). The thermal voltage is calculated from the equation (Hansen et al. 2000; Qi and Ming 2012):

$$V_t = \frac{kT}{q}, \quad (2)$$

where  $q$  is the charge of an electron ( $= 1.592 \times 10^{-19} \text{ Coulomb}$ ),  $k$  is the Boltzmann constant ( $= 1.38 \times 10^{-23} \text{ Joules/Kelvin}$ ), and  $T$  is the solar cell temperature (in Kelvin).

The PV arrays are composed of several series and parallel connected PV cells. Cells connected in parallel increase the current and cells connected in series provide greater output voltages. If there are  $N_s$  cells connected in series

in the PV array, then the thermal voltage of the array is given by (Villalva et al. 2009):

$$V_{t,n} = N_s \left( \frac{kT}{q} \right). \quad (3)$$

The thermal voltage  $V_{t,n}$  is known as the thermal voltage of  $N_s$  series-connected cells at the temperature  $T$ . If the array is composed of  $N_p$  parallel connections of cells then the photocurrent and the saturation current can be expressed as (Villalva et al. 2009):

$$\begin{cases} I_{L,n} = N_p I_L, \\ I_{0,n} = N_p I_0. \end{cases} \quad (4)$$

The photocurrent  $V_{t,n}$  and the saturation current  $I_{0,n}$  are known as the photocurrent and the saturation current of  $N_p$  parallel-connected cells in the array. In order to model power generation of the PV array, it is sufficient to model for the PV cell. Thus, we study the power generation modelling of the PV cell and the effect of temperature variations on its characteristic curves.

By Kirchhoff law, the net source current of the cell delivered to the external load equals the photocurrent,  $I_L$ , less the diode current  $I_d$ , and the ground shunt current, i.e.,

$$I = I_L - I_d - I_{sh}. \quad (5)$$

If  $V$  is the net output voltage, then by Ohm's law, we have

$$I_{sh} = \frac{(V + IR_s)}{R_{sh}}. \quad (6)$$

From Eq. (1), (5), and (6), we get

$$I = I_L - I_0 \left[ \exp\left(\frac{V}{aV_t}\right) - 1 \right] - \left[ \frac{V + IR_s}{R_{sh}} \right]. \quad (7)$$

The last term in Eq. (7) is the ground leakage current. In practical cells, it can be ignored since it is negligible compared to  $I_L$  and  $I_d$  (Patel 2005). Then, Eq. (7) takes the following form:

$$I = I_L - I_0 \left[ \exp\left(\frac{V}{aV_t}\right) - 1 \right]. \quad (8)$$

The short circuit current,  $I_{sc}$  of the PV cell is obtained by setting  $V = 0$  in Eq. (8) which leads  $I_{sc} = I_L$ . The photocurrent,  $I_L$  in Eq. (8) depends on the irradiance intensity,  $G$  (Watt/meter<sup>2</sup>) and the cell temperature,  $T$ , which can be expressed as (Walker 2001; Qi and Ming 2012):

$$I_L = \frac{G}{G_{ref}} \left[ I_{sc,ref} + \alpha_{I_{sc,ref}} (T - T_{ref}) \right], \quad (9)$$

where  $G_{ref}$  is the reference irradiance intensity ( $G_{ref} = 1000$  Watt/meter<sup>2</sup>),  $T_{ref}$  is the reference temperature ( $T_{ref} = 25^\circ\text{C}$ ),  $I_{sc,ref}$  is the cell short-circuit current at reference condition, and  $\alpha_{I_{sc,ref}}$  is the solar cell short-circuit temperature coefficient (Ampere/Kelvin) which is defined as (Soto et al. 2006):

$$\alpha_{I_{sc,ref}} = \left( \frac{I_{sc} - I_{sc,ref}}{T - T_{ref}} \right). \quad (10)$$

The ratio  $\frac{G}{G_{ref}}$  is known as the solar intensity, i.e.,

$$g := \frac{G}{G_{ref}}. \quad (11)$$

Then, Eq. (9) can be rewritten as:

$$I_L = g \left[ I_{sc,ref} + \alpha_{I_{sc,ref}} (T - T_{ref}) \right]. \quad (12)$$

For the reverse saturation current,  $I = 0$ ,  $I_L = I_{sc}$ , and  $V = V_{oc}$ , where  $V_{oc}$  is the cell's open-circuit voltage. Thus, from Eq. (8), the reverse saturation current at the reference condition,  $I_{0,ref}$  can be obtained as:

$$I_{0,ref} = \frac{I_{sc,ref}}{\left[ \exp\left(\frac{V_{oc,ref}}{aV_{t,ref}}\right) - 1 \right]}, \quad (13)$$

where  $V_{oc,ref}$ , and  $V_{t,ref}$  are the cell open-circuit voltage, and the thermal voltage at the reference condition, respectively.

Further, the reverse saturation current,  $I_{0,ref}$ , at the reference condition can be expressed as (Messenger and Ventre 2004; González-Longatt 2005; Qi and Ming 2012):

$$I_{0,ref} = Q \left( T_{ref} \right)^{\frac{3}{a}} \exp \left( \frac{E_b}{aV_{t,ref}} \right), \quad (14)$$

where  $Q$  is the semiconductor-material dependent constant, and  $E_b$  is band-gap energy in the solar cell ( $E_b = 1.12$  to  $1.15\text{eV}$ ). Similarly, the reverse saturation current,  $I_0$ , at the temperature,  $T$  is given by:

$$I_0 = Q \left( T \right)^{\frac{3}{a}} \exp \left( \frac{E_b}{aV_t} \right), \quad (15)$$

The ratio of Eq. (14) and Eq. (15) gives

$$I_0 = I_{0,ref} \left( \frac{T}{T_{ref}} \right)^{\frac{3}{a}} \exp \left[ \left( \frac{qE_b}{ak} \right) \left( \frac{1}{T} - \frac{1}{T_{ref}} \right) \right]. \quad (16)$$

Combining Eq. (13) and (16), the reverse saturation current,  $I_0$ , at the operating temperature  $T$  can be rewritten as:

$$I_0 = \frac{I_{sc,ref}}{\left[ \exp \left( \frac{V_{oc,ref}}{aV_{t,ref}} \right) - 1 \right]} \left( \frac{T}{T_{ref}} \right)^{\frac{3}{a}} \exp \left[ \left( \frac{qE_b}{ak} \right) \left( \frac{1}{T} - \frac{1}{T_{ref}} \right) \right]. \quad (17)$$

The open circuit current,  $V_{oc}$  of the cell is obtained when the load current is zero and is given by (González-Longatt 2005):

$$V_{oc} = V + IR_s. \quad (18)$$

The Series resistance  $R_s$  is included in order to cater for the losses that exist in the cells and between the cells in the array. The expression of  $R_s$  for the open-circuit voltage at the reference condition can be obtained as (González-Longatt 2005; Awodugba et al. 2013):

$$R_s = - \left( \frac{dV}{dI_{V_{oc,ref}}} \right) - \frac{1}{\left( \frac{I_{0,ref}}{aV_{t,ref}} \right) \exp \left( \frac{V_{oc,ref}}{aV_{t,ref}} \right)}. \quad (19)$$

At the open-circuit condition  $V = V_{oc}$ , the net source current given by Eq. (8) is expressed as (Villalva et al. 2009; Bellia et al. 2014):

$$I = I_L - I_0 \left[ \exp \left( \frac{V_{oc}}{aV_t} \right) - 1 \right]. \quad (20)$$

Eq. (20) is also written in the form:

$$I = I_L - I_0 \left[ \exp \left( \frac{q(V + IR_s)}{akT} \right) - 1 \right], \quad (21)$$

where  $I_L$ ,  $I_0$ , and  $R_s$  are computed using Eq. (12), Eq. (17), and Eq. (19), respectively.

Manufacturers typically provide operational data for photovoltaic panels, such as the open circuit voltage ( $V_{oc}$ ), the short circuit current ( $I_{sc}$ ), the temperature coefficients at short circuit current ( $\alpha_{I_{sc,ref}}$ ), and the nominal operating cell temperature etc (Soto et al. 2006). The PV cell conversion efficiency is sensitive to small variations in  $R_s$ . A small increase in  $R_s$  can decrease the PV output significantly (Patel 2005). The behaviour of the solar cell is modeled using Eq. (21) and either a voltage or current set by the solar array interface and then solving for the corresponding current or voltage respectively. The well known Newton-Raphson method is used to solve Eq. (21) numerically.

### 3. RESULTS AND DISCUSSION

Newton-Raphson method is a method for finding successively better approximations of the roots of a function; given a function  $f(x)$ , its derivative  $f'(x)$ , and initial guess  $x_i$ , Newton-Raphson method gives the next guess,  $x_{i+1}$ , as:

$$x_{i+1} = x_i - \frac{f(x_i)}{f'(x_i)}, i = 0, 1, 2, 3, \dots \quad (22)$$

In order to use Newton-Raphson method to solve Eq. (21), it must be transformed into a different function so that the solution to Eq. (21) is the root of the new function. This is done simply by subtracting  $I$  from both sides giving:

$$f(x) \equiv I_L - I_0 \left[ \exp \left( \frac{q(V + IR_s)}{akT} \right) - 1 \right] - I. \quad (23)$$

Above function can now be used with Newton-Raphson method to solve for  $V$  or  $I$  given  $I$  or  $V$ , respectively, once the respective derivative,  $f'(V)$  or  $f'(I)$ , is found. Having computed either  $V$  or  $I$  from Newton-Raphson method, the power produced by the PV device is the product of the current and voltage:

$$P = V * I. \quad (24)$$

Fig. 3 depicts  $I-V$  characteristic curve variation when the cell is fully, partially, and not illuminated by the Sun at a fixed reference temperature. We have chosen the diode quality factor,  $\alpha = 1.2$ , the reference temperature  $T_{ref} = 25^{\circ}\text{C}$ ,  $V_{oc}(T_{ref}) = 0.665\text{V}$ ,  $I_{sc}(T_{ref}) = 5.75\text{Ampere}$ ,

$$\alpha_{I_{sc,ref}} = 0.0035\text{Ampere/Kelvin}, \frac{dV}{dI_{V_{oc}}} = -0.00985$$

Voltage/Ampere, and  $E_g = 1.12\text{eV}$  (González-Longatt 2005). From Fig. 3, it can be seen that when the Sun is fully illuminated on the cell, it generates more current. The current generation decreases when the Sun moves from full to partial illumination condition and there is no current generation when the cell is in eclipse. Figs. 4 and 5 show  $P-V$  and  $P-I$  characteristic curve variations when the cell is in full, partial, and not illuminated conditions at  $T_{ref} = 25^{\circ}\text{C}$ . From Figs. 4-5, it can be seen that maximum power is generated when the Sun is fully illuminated on the solar cell while it decreases towards partial illumination and becomes zero when there is no Sun illumination on the cell.

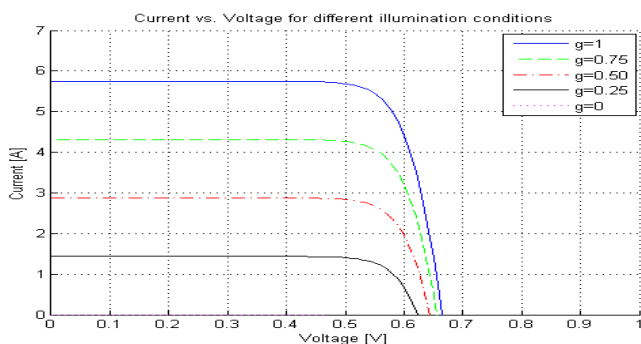


**Fig. 3:** Voltage vs. current when the Sun is fully ( $g = 1$ ), partially ( $0 < g < 1$ ), and not illuminated ( $g = 0$ ) at  $T_{ref} = 25^{\circ}\text{C}$  on PV cell.

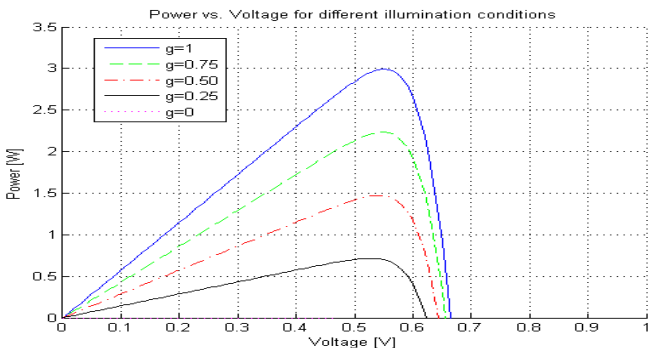


**Fig. 4:** Power vs. voltage when the Sun is fully ( $g = 1$ ), partially ( $0 < g < 1$ ), and not illuminated ( $g = 0$ ) at  $T_{ref} = 25^{\circ}\text{C}$  on PV cell.

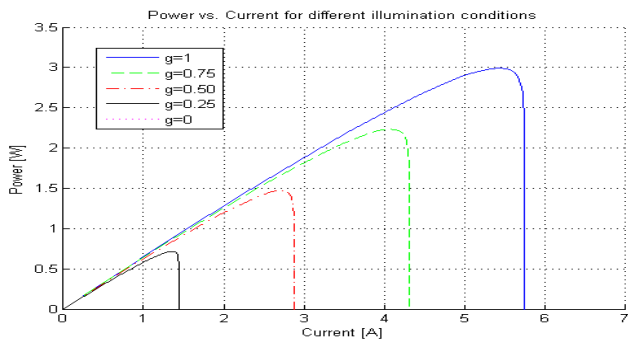


**Fig. 5:** Power vs. current when the Sun is fully ( $g = 1$ ), partially ( $0 < g < 1$ ), and not illuminated ( $g = 0$ ) at  $T_{ref} = 25^{\circ}\text{C}$  on PV cell.

The effect of temperature variations on the characteristic curves are shown in Figs. 6-11. Figs. 6 and 7 depict  $I-V$  curves of a solar cell when the Sun is fully ( $g = 1$ ) and partially ( $g = 0.5$ ) illuminated, respectively at different temperatures,  $0^{\circ}\text{C}$ ,  $25^{\circ}\text{C}$ ,  $50^{\circ}\text{C}$  and  $75^{\circ}\text{C}$  on the cell. Figs. 8 and 9 show  $P-V$  curves while Figs. 10 and 11 depict  $P-I$  curves, respectively when the Sun is fully and partially illuminated at  $0^{\circ}\text{C}$ ,  $25^{\circ}\text{C}$ ,  $50^{\circ}\text{C}$  and  $75^{\circ}\text{C}$ . From Figs. 6 and 7, it can be observed that with increasing temperature, the current of the cell increases whereas the voltage decreases. We observe that the increase in current is much less than the decrease in voltage, hence the net effect is the decrease in power with increasing temperature which is shown in Figs. 8-11 for both fully and partially illuminated conditions on the cell.

#### 4. CONCLUSIONS

In this work, the spacecraft power generation modeling is carried out. The modeled characteristic equation of the solar cell is solved by Newton-Raphson method. The characteristic curves for  $I-V$ ,  $P-V$ ,  $P-I$  at different

temperatures are shown when the Sun is in full, partial and not illuminated conditions on the cell. We observe that when the Sun is fully illuminated on the cell, it generates more current. The current generation decreases when the Sun moves from full to partial illumination and there is no current generation when there is eclipse on the cell. The maximum power is generated when the Sun is fully illuminated on the cell while it decreases towards partial illumination condition and becomes zero when there is no Sun illumination on the cell. It is observed that with increasing temperature, the current of the cell increases whereas the voltage decreases. The increase in current is much less than the decrease in voltage; hence the net effect is the decrease in power with increasing temperature.

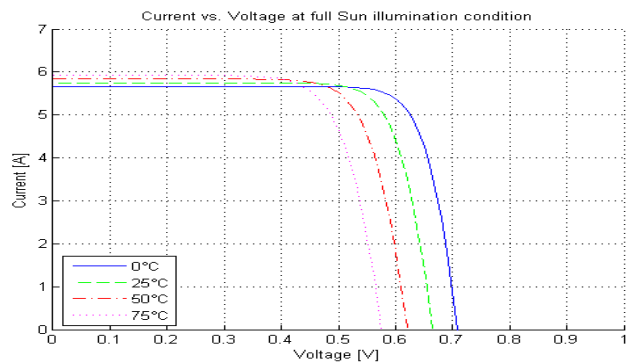


**Fig. 6:** Current vs. voltage variation when the Sun is fully illuminated ( $g = 1$ ) at different temperatures.

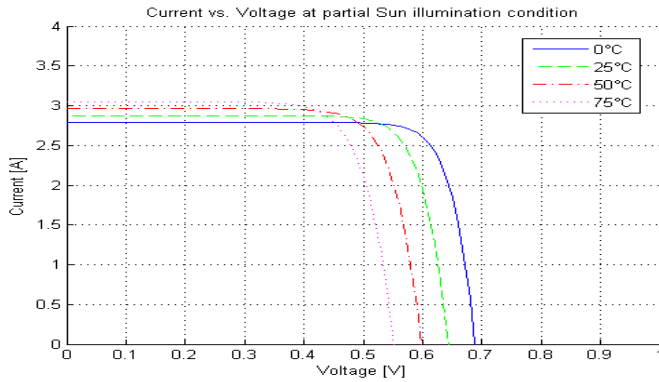


**Fig. 7:** Current vs. voltage when the Sun is partially illuminated ( $g = 0.5$ ) at different temperatures.

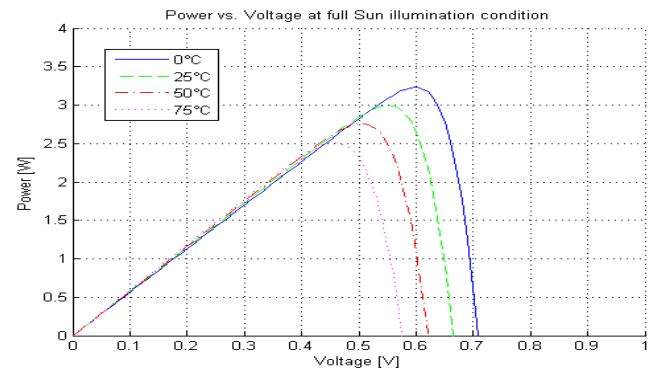


**Fig. 8:** Power vs. voltage variation when the Sun is fully illuminated ( $g = 1$ ) at different temperatures.

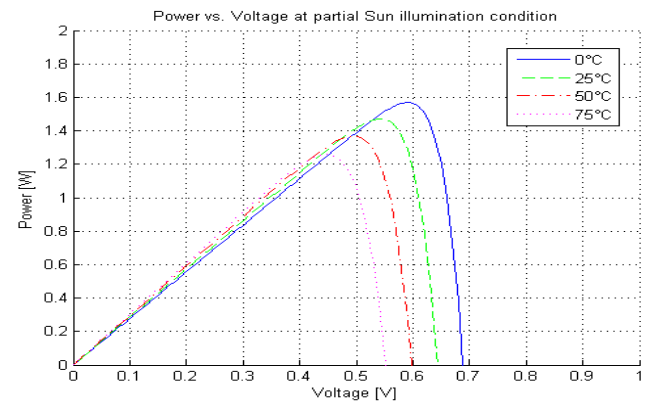


**Fig. 9:** Power vs. voltage variation when the Sun is partially illuminated ( $g = 0.5$ ) at different temperatures.

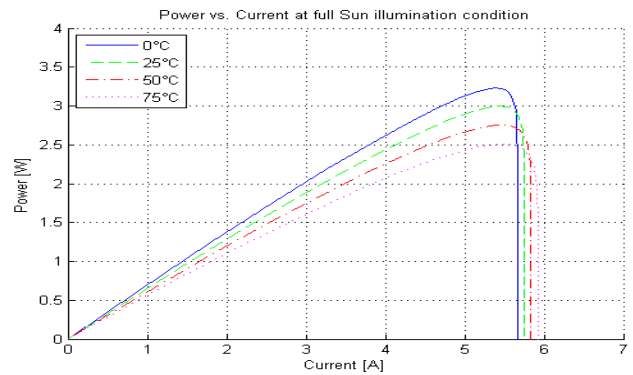


**Fig. 10:** Power vs. current variation when the Sun is fully illuminated ( $g = 1$ ) at different temperatures.

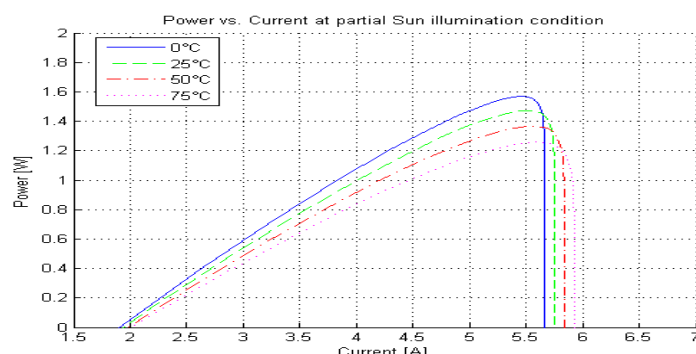


**Fig. 11:** Power vs. current variation when the Sun is partially illuminated ( $g = 0.5$ ) at different temperatures.

## REFERENCES

- [1] M. Patel, Spacecraft Power Systems. Boca Raton, USA: CRC Press, 2005.
- [2] F.J. G. Sanchez, I.O. Conde, J.J. Liou, "Parasitic series resistance-independent method for device model parameter extraction," IEEE Proc. Circuits Devices Syst., vol. 143, no. 1, pp. 68-70, Apr. 1996.
- [3] A. D. Hansen, P. Sørensen, L. H. Hansen, H. Bindner "Models for a Stand-Alone PV System," Risø National Laboratory Technical Report-R-1219(EN) / SEC-R-12, Dec 2000, Risø National Laboratory for Sustainable Energy, Risø, Denmark.
- [4] G. Walker, "Evaluating MPPT converter topologies using a MATLAB PV model," Journal of Electrical and Electronics Engineering, Australia, vol.21, No. 1, 2001, pp.49-56.
- [5] R. A. Messenger, J. Ventre, 2004. Photovoltaic Systems Engineering, second ed. CRC Press LLC, Boca Raton, FL.
- [6] F. M. González-Longatt, "Model of photovoltaic module in Matlab," in 2do congreso iberoamericano de estudiantes de ingeniería en electrónica, electrónica y computación, ii cibelec, 2005, pp. 1-5.
- [7] W. De Soto, S.A. Klein, W.A. Beckman, "Improvement and validation of a model for photovoltaic array performance," Solar Energy, Vol. 80, 2006, pp. 78-88.
- [8] M. G. Villalva, J. R. Gazoli, E. R. Filho, "Comprehensive Approach to Modeling and Simulation of Photovoltaic Arrays," IEEE Transactions on Power Electronics, Vol. 24, No. 5, 2009, pp. 1198-1208.
- [9] Chen Qi, Zhu Ming, "Photovoltaic Module Simulink Model for a Stand-alone PV System," Physics Procedia, Vol. 24, 2012, pp. 94-100.
- [10] S. G. Pachpande, P. H. Zope, "Studying the effect of shading on Solar Panel using MATLAB," International Journal of Science and Applied Information Technology, Vol. 1, No. 2, 2012, pp. 46-51.
- [11] A. O. Awodugba, Y. K. Sanusi, J. O. Ajayi, "Photovoltaic solar cell simulation of shockley diode parameters in matlab," International Journal of Physical Sciences, Vol. 8, No. 22, 2013, pp. 1193-1200.
- [12] H. Bellia, R. Youcef, M. Fatima, "A detailed modeling of photovoltaic module using MATLAB," NRIAG Journal of Astronomy and Geophysics, Vol. 3, 2014, 53-61.
- [13] V.K. Srivastava, Ashutosh, M. Pitchaimani, B.S. Chandrasekhar, Eclipse Prediction Methods for LEO satellites with Cylindrical and Cone geometries: A Comparative study of ECSM and ESCM to IRS satellites, Astron. Comput., Vol. 2, 2013, pp. 11-17.
- [14] V. K. Srivastava, Ashutosh, M. V. Roopa, B. N. Ramakrishna, M. Pitchaimani, B. S. Chandrasekhar, Spherical and Oblate Earth conical Shadow models for LEO satellites: Applications and comparisons with real time data and STK to IRS satellites, Aerosp. Sci. Technol. Vol. 33, 2014, pp. 135-144.
- [15] V. K. Srivastava, S. M. Yadav, Ashutosh, J. Kumar, B. S. Kushvah, B. N. Ramakrishna, P. Ekambaram, Earth conical shadow modeling for LEO satellite using reference frame transformation technique: A comparative study with existing earth conical shadow models, Astron. Comput., Vol. 9, 2015a, pp. 34-39.
- [16] V.K. Srivastava, J. Kumar, S. Kulshrestha, A. Srivastava, M.K. Bhaskar, B.S. Kushvah, P. Shiggavi, D.A. Vallado, Lunar shadow eclipse prediction models for the Earth orbiting spacecraft: Comparison and application to LEO and GEO space crafts, Acta Astronautica, Vol. 110, 2015b, pp. 206-213.
- [17] V.K. Srivastava, J. Kumar, S. Kulshrestha, B.S. Kushvah, M.K. Bhaskar, Somesh S., M.V. Roopa, B.N. Ramakrishna, Eclipse Modeling for the Mars Orbiter Mission, Advances in Space Research, Vol. 56, No. 4, 2015c, pp. 671-679.
- [18] S. Kulshrestha, M.K. Bhaskar, Moon shadow eclipse prediction of a lunar orbiting spacecraft, Vol. 2, No. 4, 2015, pp. 1545-1548.

## BIOGRAPHIES



Mrs. Shivali Kulshrestha has done B.E. in Electrical Engineering from JECRC, Jodhpur, India. Currently, she is pursuing M.E. in Electrical Engineering with specialization in power system from M.B.M. Engineering College, J.N.V. University, Jodhpur, India.



Dr. M.K. Bhaskar is currently working as an associate professor in Electrical Engineering, M.B.M. Engineering College, J.N.V. University, Jodhpur, India.